Alemán, Christian; Busch, Christopher; Ludwig, Alexander; Santaeulàlia-Llopis, Raül

Working Paper

Evaluating the effectiveness of policies against a pandemic

SAFE Working Paper, No. 294

Provided in Cooperation with:
Leibniz Institute for Financial Research SAFE

Suggested Citation: Alemán, Christian; Busch, Christopher; Ludwig, Alexander; Santaeulàlia-Llopis, Raül (2020) : Evaluating the effectiveness of policies against a pandemic, SAFE Working Paper, No. 294, Leibniz Institute for Financial Research SAFE, Frankfurt a. M., https://doi.org/10.2139/ssrn.3714697

This Version is available at:
https://hdl.handle.net/10419/226212

Christian Alemán | Christopher Busch | Alexander Ludwig |
Raül Santaeulália-Llopis

Evaluating the Effectiveness of Policies Against a Pandemic

SAFE Working Paper No. 294

Leibniz Institute for Financial Research SAFE
Sustainable Architecture for Finance in Europe
info@safe-frankfurt.de | www.safe-frankfurt.de

Evaluating the Effectiveness of Policies Against a Pandemic*

Christian Alemán† Christopher Busch‡ Alexander Ludwig§
Raül Santaeulàlia-Llopis¶

November 11, 2020

Abstract

We develop a novel empirical approach to identify the effectiveness of policies against a pandemic. The essence of our approach is the insight that epidemic dynamics are best tracked over *stages*, rather than over time. We use a normalization procedure that makes the pre-policy paths of the epidemic identical across regions. The procedure uncovers regional variation in the *stage* of the epidemic at the time of policy implementation. This variation delivers clean identification of the policy effect based on the epidemic path of a leading region that serves as a counterfactual for other regions. We apply our method to evaluate the effectiveness of the nationwide stay-home policy enacted in Spain against the Covid-19 pandemic. We find that the policy saved 15.9% of lives relative to the number of deaths that would have occurred had it not been for the policy intervention. Its effectiveness evolves with the epidemic and is larger when implemented at earlier stages.

Keywords: Macroeconomics, Pandemic, Stages, Covid-19, Stay-Home, Policy Effects, Identification
JEL Classification: E01, E22, E25

*We thank Luca Gambetti, Dongya Koh, André Gröger, Ludo Visschers and participants of the UAB Macro Club and the Spanish Macro Network Workshop for helpful comments and suggestions.

†Universitat Autònoma de Barcelona, IDEA, and Barcelona GSE

‡Universitat Autònoma de Barcelona, MOVE, and Barcelona GSE; chris.busch@movebarcelona.eu; www.chrisbusch.eu

§Goethe University Frankfurt; SAFE; Universitat Autònoma de Barcelona, MOVE; CEPR; MEA; Netspar; ZEW; mail@alexander-ludwig.com; www.alexander-ludwig.com

¶Universitat Autònoma de Barcelona and Barcelona GSE; loraulet@gmail.com; r-santaeulalia.net

1 Introduction

In response to the worldwide Covid-19 pandemic many countries enacted a wide range of nonpharmaceutical public health policies, some of which were also implemented during earlier pandemics.[1] These policies aim to reduce interpersonal contact in order to slow down the spread of a virus and reduce its death toll. Yet, the effectiveness of the implemented measures—e.g., evaluated as the percentage of lives saved—is an open question.[2] The (typical) difficulty for the identification of the policy effect lies in establishing a counterfactual scenario that is informative about how the epidemic would have evolved had it not been for the policy intervention. This is particularly challenging when the policy is implemented nationwide at the same time (as, e.g., recently in response to the first wave of the Covid-19 epidemic in Spain), which implies that there is no cross-regional variation of the time of policy implementation—which is commonly used to identify the effects of policy.

We develop a novel empirical method to construct the counterfactual epidemic dynamics that overcomes this challenge, which builds on the notion that the dynamics of an epidemic are best tracked over *stages*, and not over time. The starting point of our method is the observation that at a given point in time there is potential heterogeneity across regions in terms of how far they moved along an epidemic path. We illustrate this phenomenon in panel (a) of Figure 1 which shows a stylized epidemic path in terms of the daily flow of deaths associated with the epidemic.[3] Assume that two regions go through that path. If the epidemic starts earlier in region $\mathcal{C}$ than in region $\mathcal{T}$, then at some calendar date t, the epidemic will be more advanced in region $\mathcal{C}$—we refer to this as a more advanced *stage* of the epidemic. We use this heterogeneity of region-specific epidemic *stages* at the time of policy implementation to identify the effects of policy.

In practice, there is not only heterogeneity in the calendar date at which an epidemic starts, because regions will not go through an identical path once the regional epidemic is initiated. Instead, epidemics can differ across regions in several dimensions—in particular, the speed of

[1] These policies include unprecedented lockdown measures that often implied some kind of stay-home (or shelter-in-place) orders, school closures, restrictions on business opening hours, enforcement of hygiene protocols in public spaces etc. For example, during the 1918 influenza pandemic (commonly known as the Spanish flu), the New York City health commissioner ordered businesses to open and close on staggered shifts to prevent overcrowding on the public transport.

[2] For example, if a stay-home policy is implemented before an epidemic starts to spread through the population, then such a policy is—arguably—drastic but unambiguously effective at saving lives. On the contrary, if the policy is enacted when the path of infections is complete, then stay-home policies will be unambiguously irrelevant. For the practical example of stay-home policies enacted against Covid-19, since infections were in course at the time at which stay-home policies were implemented, the true effectiveness of the these policies against the epidemic is likely to be in between these two exemplified extremes.

[3] Our notion of stages is continuous, and can thus also be thought of as an extension of the discrete epidemic intervals defined by the CDC in its Updated Preparedness and Response Framework for Influenza Pandemics (CDC, 2014). According to the CDC framework, the stylized epidemic path in Figure 1 can be segmented into *initiation* (where the flow takes off), *acceleration* (up to the peak), and *deceleration* (after the peak).

Figure 1: The Evolution of an Epidemic: An Illustration with Two Regions

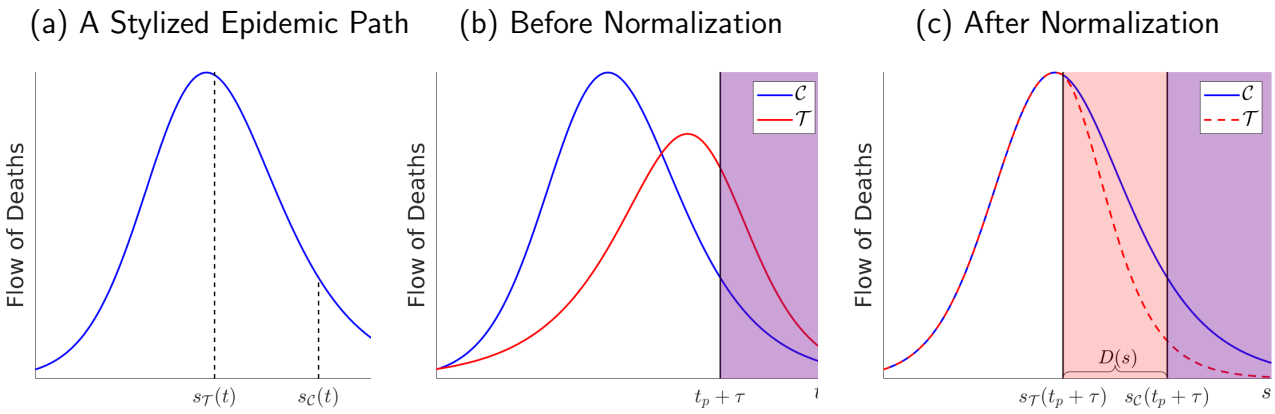

Notes: Panel (a) shows a stylized epidemic path where $s_{\mathcal{C}}(t)$ and $s_{\mathcal{T}}(t)$ denote the stage at time t of regions $\mathcal{C}$ and $\mathcal{T}$, respectively; panel (b) shows two different epidemic paths for regions $\mathcal{C}$ and $\mathcal{T}$ as a function of time t, where period $t_p + \tau$ is the time period when a policy implemented in period t_p becomes effective with time lag τ; and panel (c) shows the same epidemic paths after normalizing the epidemic of region $\mathcal{T}$ onto region $\mathcal{C}$. The orange shaded area in Panel (c) is the overlap interval $D(s)$—defined over stages of the epidemic—in which region $\mathcal{T}$ is affected by the policy, whereas region $\mathcal{C}$ is not.

disease diffusion, and the magnitude (or overall death toll). To illustrate these dimensions, in panel (b) of Figure 1 we show the time-path of the epidemic of two example regions. The epidemic starts earlier, evolves faster, and has a larger magnitude in region $\mathcal{C}$ than in region $\mathcal{T}$. Importantly, there is a wide range of factors—some of which might be unobserved—that potentially determine the differential epidemic paths across regions: among others, differences in the degree of network connectivity with off-region infected individuals (or clusters) can determine differences in the dates at which the epidemics start; cultural (or other) differences in the extent of interpersonal physical contact at work, commuting or socializing, the age composition and health distribution of the population, and environmental factors such as air pollution can explain the differential speed at which the epidemic diffuses across populations. Clearly, a warranted assessment of the effects of policy needs to control for these factors in a comprehensive manner. In an ideal scenario—absent any differences in the observed and unobserved factors that determine the epidemic—the epidemic path of any two regions is identical before policy implementation. The empirical method that we develop achieves this goal without having to single out the forces that drive the epidemic.

Our identification consists of normalizing the time, speed and magnitude of the epidemic paths across regions. In particular, the normalization ensures that before the policy is implemented all regions share the same normalized epidemic path. We illustrate this normalization in panel (c) of Figure 1 where we normalize the epidemic path of region $\mathcal{T}$ onto the epidemic path of region $\mathcal{C}$ before policy affects the epidemic. In terms of reducing deaths, a policy implemented in period t_p

becomes effective with time lag τ in both regions and, hence, $t_p + \tau$ is the effective policy date.[4] Then, since region $\mathcal{T}$ lags region $\mathcal{C}$, the calendar date $t_p + \tau$ corresponds to an earlier *stage* in region $\mathcal{T}$ than in region $\mathcal{C}$—making region $\mathcal{C}$ a suitable candidate for a control region and $\mathcal{T}$ for a treatment region. Put differently, our normalization unveils differences in the *stage* of the epidemic across regions at the time of policy implementation that we exploit to identify the policy effect. In particular, there exists an overlap interval $D(s)$—defined between *stages* $s_{\mathcal{T}}(t_p + \tau)$ and $s_{\mathcal{C}}(t_p + \tau)$—within which the epidemic path in region $\mathcal{T}$ is affected by the policy whereas the epidemic path of region $\mathcal{C}$ continues to evolve without policy intervention. This overlap interval is illustrated by the orange shaded area in panel (c) of Figure 1. We use the difference between the normalized paths of the epidemics over this overlap interval to estimate the policy effect.

We apply our method to quantify the effectiveness of the stay-home policy enacted against the Covid-19 epidemic in Spain. On March 14, 2020, the Spanish government announced a nationwide stay-home policy—enacted the following day—that locked down all non-essential workers in each and all regions of Spain. We find that the epidemic in Madrid leads the ones in other regions, and thus at the time of policy implementation Madrid was at a later epidemiological *stage* than the rest of the country. Hence, we use Madrid as our control region that gives the counterfactual epidemic for the rest of Spain—an artificial region that consists of Spain without Madrid. As in our above stylized example, we find an overlap interval—of one week—in terms of the *stages* of the epidemic during which the rest of Spain was treated with the stay-home policy, whereas Madrid was not.

Our results imply that during this overlap interval 18.7% of people that would have died had it not been for the policy were saved in Spain—without Madrid. We refer to this as the percentage of lives saved. Accordingly, in the first week the stay-home policy became effective about 1,074 lives were saved. We also calculate the implied number of lives saved after the overlap interval assuming that the percentage difference of daily deaths is the same as on the overlap interval. This gives an estimate of the total number of lives saved due to implementing the stay-home policy. Precisely, the stay-home policy that run from March 15 to May 2—i.e. until the first wave of the epidemic flattened out and the strictest measures were lifted, saved about 19.4% of lives—or 3,787 lives—in Spain without Madrid.[5]

[4] The policy does not necessarily have an immediate effect on the flow of deaths because the process from infection to death occurs with some lag $\tau \geq 0$. In the case of Covid-19 it takes on average between twelve to twenty-three days from infection to death, as reported by the Instituto de Salud Carlos III (ISCIII); see `isciii.es`. Therefore, the effective policy date is $t_p + \tau$ and not the date of policy implementation t_p. In our analysis, we choose a benchmark of $\tau = 12$ corresponding to the lower bound reported by ISCIII. We conduct robustness with values of τ that are above and below our benchmark choice.

[5] Our benchmark results are based on the official measurement of Covid-19 deaths in Spain —i.e. deaths that tested positive for Covid-19 using PCR tests. We also conduct our analysis on excess deaths data, which in principle also captures additional deaths that are indirectly happening due to Covid-19. We find effects of policy of similar size to our benchmark results; see our Section 4.3.

We also explore how the effects of policy differ over the course of the epidemic. To this end, we split Spanish regions into three subgroups by their epidemic stage at the effective policy date and then separately estimate the effectiveness of policy. We find that the regions for which the stay-home policy was implemented at earlier stages show larger policy effectiveness than regions for which the policy was implemented at later stages: during the overlap interval 33.2% of lives saved for early implementers and 8.2% for late implementers. This drop in policy effectiveness occurs rather rapidly—in terms of stages, the early implementers enter policy about one week earlier than the late implementers. That is, a delay of one week in the introduction of the policy drops effectiveness by approximately three fourths. Importantly, this is not a purely mechanical effect due to a longer overlap interval, but also stems from a larger estimated proportion of lives saved per day. Finally, we extrapolate our estimates to the time series of daily deaths in Madrid—the latest implementer. By our extrapolation, we attribute 4.1% of lives saved to the implementation of stay-home policies for the entire first wave of the epidemic. Aggregating Madrid to the rest of Spain translates into a total of 4,024 lives saved which corresponds to an effectiveness of 15.9% of lives saved in Spain. Again, this percentage refers to the counterfactual stock of deaths that would have occurred had it not been for the observed policy intervention.

Our work relates to three stands of literature. First, our normalization of the epidemic relates to previous work in Iorio and Santaeulàlia-Llopis (2016) that explores the relationship between education and the probability of being infected with HIV over the course of the epidemic. In that context, country-specific HIV epidemic paths are normalized to an aggregate path in order to define stages of the epidemic in a comparable manner across time and space. We depart from that work in that we use the normalization of the epidemic as base for identifying the effects of policies that aim to alter the path of the epidemic itself. This implies the normalization of pre-policy epidemic paths across suitable control and treatment regions. More generally, our notion of epidemic stages is also analogous to the stylized stages of economic development (e.g., Lucas 2004) and the demographic transition (e.g., Galor and Weil 2000, Greenwood et al. 2005, Cervellati and Sunde 2015, and Delventhal et al. 2019).

Second, our work relates to research that empirically assesses the effectiveness of policy interventions aiming at containing pandemics. Similarly in spirit to our analysis, which is agnostic about the exact mechanisms driving the epidemic, Dave et al. (2020) use a synthetic control (SC) group approach developed in Abadie and Gardeazabal (2003) and Abadie et al. (2010).[6] In this context, we view our approach as preferable for our research question for several reasons. First, the SC assigns weights—based on observable variables—to regions that did not implement the

[6]One alternative is to model the epidemic, for example by variants of an SEIR (susceptible-exposed-infected-recovered) model, which is a set of differential equations describing the dynamics of an epidemic. A prominent example in this spirit is Bootsma and Ferguson (2007), who evaluate policies during the 1918 influenza pandemic—and who construct counterfactual dynamics by means of such SEIR models.

policy such that the resulting pre-policy time path of the epidemic of a SC region is similar to the path of the treatment region. This implies that issues related to time-varying unobservables are not addressed by the SC approach. Our approach overcomes these issues by generating the exact same pre-policy time paths for the control and treatment regions regardless of what factors—including unobservables—drive the epidemic. Second, feasibility. The SC approach relies on some suitable control regions not experiencing policy treatment at the time of policy implementation. Hence, SC cannot be used to assess stay-home policies that are implemented nationwide at the same calendar date. Our approach is also suitable when all regions experience policy treatment at the same date, such as in our case study for Spain. Third, the SC group approach relies on the assumption that the epidemic dynamics in the control regions do not change when policy is introduced in the treatment region. This precludes endogeneity of behavior relevant to the spread of the virus with respect to policy treatment in another region. Our approach does not require such assumptions: the studied policy is introduced on the same calendar date, and the counterfactual dynamics of the control region are based on data from before this date. Fourth, the SC group approach (implicitly) assumes that control and treatment regions are at the same *stage* of the epidemic at the time of policy implementation. However, in practice, we observe that regions differ in their epidemiological *stage* at the time of policy implementation. Our approach is explicitly designed to exploit this variation in epidemic *stages* across regions to provide identification.

Finally, our work directly relates to the macroeconomic literature on optimal lockdown. An essential aspect of this literature is the trade-off between economic loss (including social costs) and lives saved by stay-home policies (e.g., Alvarez et al. 2020, Atkeson 2020, Barro et al. 2020, Eichenbaum et al. 2020, Farboodi et al. 2020, Fogli et al. 2020, Glover et al. 2020, Kaplan et al. 2020, Piguillem and Shi 2020, among others). In this context, the measurement of how many lives are saved by stay-home policies is of first-order importance. Our estimates provide an empirically grounded measure of the effectiveness of these policies in reducing the death toll of the epidemic and, for this reason, our results should be informative for the calibration and estimation of policy parameters in models of the epidemic. Further, note that the empirical nature of our approach allows us to be agnostic with respect to the driving forces of the epidemic dynamics.[7] Hence, our results are informative for any model of the epidemic, independently of the theoretical mechanisms that generate the epidemic which might differ across models.

The rest of the paper is structured as follows. Section 2 discusses our approach to identification of the effectiveness of policy interventions. Section 3 discusses the evolution of the epidemic and policy timeline in Spain. Section 4 shows the average effects of policy and over the course of the epidemic in Spain. Section 5 concludes.

[7] That is, our results do not hinge on any assumptions regarding the deep parameters embedded in epidemic models.

2 Identifying the Effectiveness of Policy

In this section, we first discuss the identification of the policy effect in an ideal (hypothetical) scenario where a (public health) policy is introduced on an epidemic path. We then show how empirically observed epidemic dynamics can be normalized to resemble this ideal scenario, and how the policy effect can be identified based on the normalized data.

Policy Effect in an Ideal Scenario. Consider a scenario in which the regional evolution of the epidemic across time is exactly the same for two regions $r \in \{\mathcal{C}, \mathcal{T}\}$ before any policy that potentially affects the epidemic is enacted. That is, these two regions are identical in every aspect relevant for the dynamics of the epidemic, such that absent any policy intervention the epidemics in the treatment region $\mathcal{T}$ and the control region $\mathcal{C}$ evolve identically. Now assume that region $\mathcal{T}$ implements a stay-home policy at some date t_p that reduces the number of epidemic deaths after date $t_p + \tau$, while the epidemic dynamics in region $\mathcal{C}$ are not affected by the policy implemented in $\mathcal{T}$. Assume further that region $\mathcal{C}$ introduces the same policy at some later date $t_p+\Delta$—reducing the flow of deaths after $t_p + \Delta + \tau$.

This scenario is ideal for two reasons. First, absent any policy intervention the epidemic evolves identically in the treatment and control regions, which implies that region $\mathcal{C}$ (before it is treated) can serve as a counterfactual for region $\mathcal{T}$. Second, at any given point in time, the two regions are at the same stage of the epidemic, which is identical to the calendar time itself, i.e., $s_{\mathcal{C}}(t) = s_{\mathcal{T}}(t) = t$. Thus, the flow of deaths in region $\mathcal{C}$ in the interval $[s_{\mathcal{T}}(t_p+\tau), s_{\mathcal{C}}(t_p+\Delta+\tau)]$ gives a counterfactual for the flow of deaths in region $\mathcal{T}$ had the policy not (yet) been introduced.

We capture the differential by a distance function $w(s;\gamma^p)$ that minimizes

$$\min_{\gamma_p} \| \ln(y_{s\mathcal{T}}) - \ln(y_{s\mathcal{C}}) - \ln(1 + w(s;\gamma^p))\|_{s=s_{\mathcal{T}}(t_p+\tau)}^{s_{\mathcal{C}}(t_p+\Delta+\tau)}, \tag{1}$$

where y_{sr} is the flow of deaths at stage s in region r, and $\|\cdot\|$ is a distance norm. The distance function $w(s;\gamma^p)$ satisfies $w(s \leq s_{\mathcal{T}}(t_p+\tau), \gamma^p) = 0$, and $\frac{\partial w(s;\gamma^p)}{\partial \gamma^p} < 0$ for $s > s_{\mathcal{T}}(t_p+\tau)$ so that when the policy is effective, a larger value of parameter γ^p means a stronger reduction in the number of deaths in the treatment group $\mathcal{T}$. We can then translate $w(\cdot)$ into the number and percentage of lives saved due to the policy during the interval in which policy is not yet introduced in the control region, and by extrapolation for the time after that interval.

Normalization of Epidemics. The previous description immediately puts at the center the challenges that are to overcome before being able to identify the policy effect based on epidemic dynamics over stages. First, if the regional epidemics in $\mathcal{C}$ and $\mathcal{T}$ start at different dates, then the epidemics are at *different stages* at a given date t. Second, across regions the virus will spread at *different speed* if the regions are not identical in every aspect relevant to the epidemic dynamics

(e.g., the population density, or the distribution of the population over age and health status). Third, and directly related, the epidemic will be of *different magnitude*, in the sense that the peak of the flow of deaths differs.

We overcome all three challenges in two steps. First, we estimate smooth functions of time t to capture the dynamics of the epidemics by region. Second, we use the estimated functions to obtain a scaling factor that adjusts for the differences in magnitude, and to find the dates t at which the epidemics in the two regions are at a given stage s (where one region serves to normalize), thereby controlling for different starting time and speed. While in the ideal scenario described above the distinction of stage s and time t is not required, it becomes crucial when across regions the epidemics evolve differently.

Now consider a scenario in which a policy is introduced at the *same date* t_p in both regions. Given the lag until the policy treatment shows an effect on the flow of deaths we refer to $t_p + \tau$ as the *effective* policy date. Our normalization procedure can handle a wide range of possible timings of the (effective) policy. Panels (a) and (b) of Figure 2 show smooth epidemics for two possible scenarios. Across both scenarios, the epidemic dynamics of each of the two regions are the same: the epidemic in region $\mathcal{C}$ starts earlier, evolves faster, and has a larger magnitude than the epidemic in region $\mathcal{T}$. In the first scenario, shown in panel (a), the effective policy date is after the respective peaks of the flows of death of the two regional epidemics. In the second scenario, panel (b), the effective policy date is before the peaks of the epidemics. In the latter case, it is possible that the policy affects the peak, and thus the magnitude, of the epidemic. Our procedure works for both cases, as well as for in-between cases where the epidemic of one region is beyond its peak, while the other is before its peak at time of policy. It is important to note that for a given date of actual policy implementation, choosing a different lag parameter τ implies choosing a different effective policy date. This is relevant for the normalization procedure insofar as we obtain normalization parameters based on (smoothed) epidemics up to the effective policy date.

For region $r \in \{\mathcal{C}, \mathcal{T}\}$ we observe the daily flow of deaths at date t as y_{tr}. Denote by $g'(t; \boldsymbol{\beta}_r)$ some continuous function fitted to those flows, and by ε_{tr} a multiplicative error term, giving

$$y_{tr} = g'(t; \boldsymbol{\beta}_r)\varepsilon_{tr}. \tag{2}$$

In other words, $g'(t; \boldsymbol{\beta}_r)$ is a smooth representation of the epidemic dynamics in region r. Importantly, the normalization procedure does not hinge on the exact form of $g'(t; \boldsymbol{\beta}_r)$: we simply need *a* continuous function estimated to capture the epidemic dynamics. If there was no measurement error, we could also directly use the observed flow data.

Figure 2: Normalization of the Epidemics: An Illustration

With Policy *After* Peak

With Policy *Before* Peak

(a) Epidemics in Control ($\mathcal{C}$) and Treatment ($\mathcal{T}$)

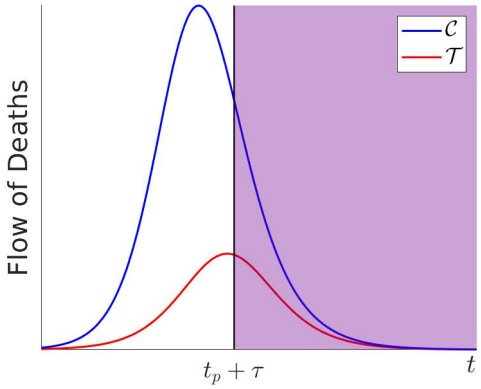

(b) Epidemics in Control ($\mathcal{C}$) and Treatment ($\mathcal{T}$)

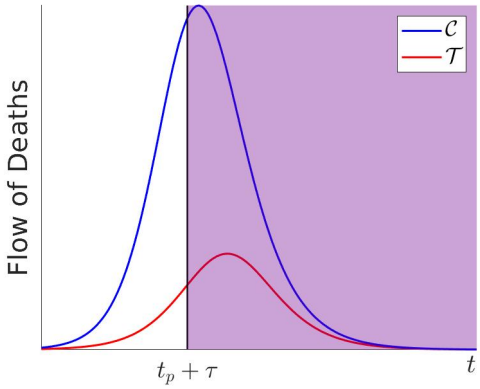

(c) Adjusting $\mathcal{T}$ for Magnitude

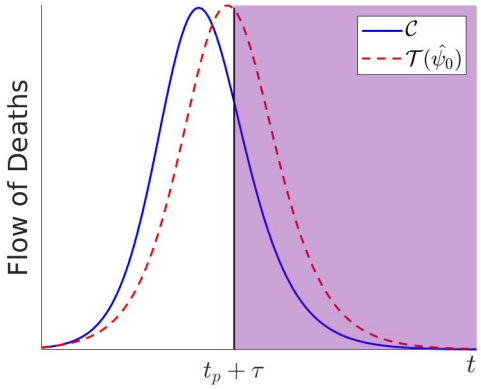

(d) Adjusting $\mathcal{T}$ for Magnitude

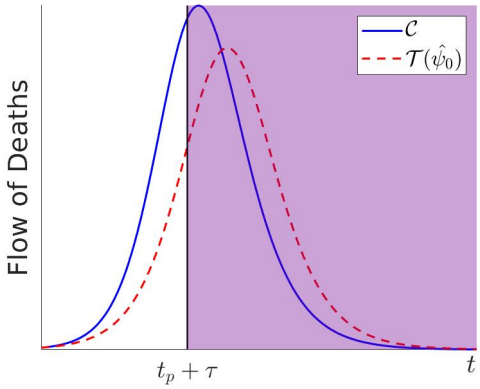

(e) Adjusting $\mathcal{T}$ for Magnitude, Time, and Speed

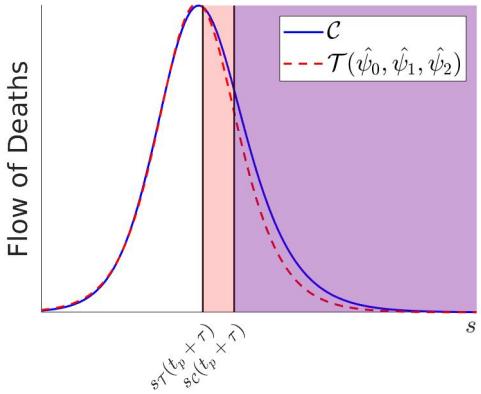

(f) Adjusting $\mathcal{T}$ for Magnitude, Time, and Speed

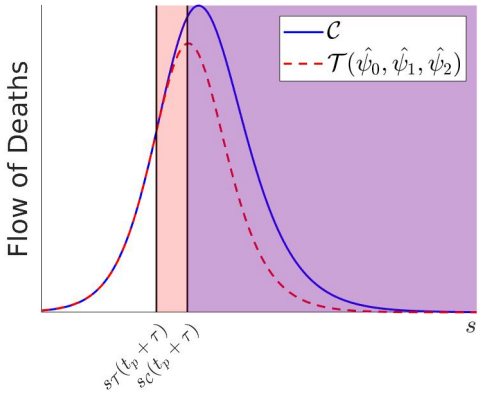

Notes: Panel (a) shows smooth epidemic dynamics represented by Generalized Logistic Functions for a control region $\mathcal{C}$ and a treatment region $\mathcal{T}$, where the policy is effective ($t_p + \tau$) after the regions reached their epidemic peaks (in terms of the death toll). Panel (c) applies the magnitude adjustment to region $\mathcal{T}$. Panel (e) additionally applies the adjustment for time and speed to region $\mathcal{T}$. Panels (b), (d), and (f) illustrate the same for a scenario where policy is effective before the epidemic peaks.

We treat region $\mathcal{C}$ as the benchmark region and define stages as[8]

$$s_r(t;\psi_1,\psi_2) = \begin{cases} s_{\mathcal{T}}(t;\psi_1,\psi_2) = \psi_1 + \psi_2 t & \text{if } r = \mathcal{T} \\ s_{\mathcal{C}} = t & \text{if } r = \mathcal{C} \end{cases} \tag{3}$$

where ψ_1 moves the epidemic forward or backwards in time, and ψ_2 adjusts its speed. We pin those down together with a scaling parameter ψ_0 that adjusts for the magnitude.

Given the fitted $g'(\cdot)$ functions, we solve for the $\boldsymbol{\psi} = \{\psi_0, \psi_1, \psi_2\}$ that minimizes the log difference of the (smoothed) epidemics on an interval up to the effective policy date:

$$\min_{\boldsymbol{\psi}} \| \ln(g'(t=s;\hat{\boldsymbol{\beta}}_{\mathcal{C}})) - \ln(\psi_0 g'(t = s_{\mathcal{T}}^{-1}(s;\psi_1,\psi_2);\hat{\boldsymbol{\beta}}_{\mathcal{T}})) \|_{s \leq s_{\mathcal{T}}(t_p+\tau;\psi_1,\psi_2)=\psi_1+\psi_2(t_p+\tau)}. \tag{4}$$

We impose two normalization conditions as constraints in the minimization:

$$\sup_{s \leq s_{\mathcal{T}}(t_p+\tau;\psi_1,\psi_2)} \psi_0 g'(t = s_{\mathcal{T}}^{-1}(s;\psi_1,\psi_2);\hat{\boldsymbol{\beta}}_{\mathcal{T}}) = \sup_{s \leq s_{\mathcal{T}}(t_p+\tau;\psi_1,\psi_2)} g'(t=s;\hat{\boldsymbol{\beta}}_{\mathcal{C}}) \tag{5a}$$

$$\psi_0 g'(t = t_p+\tau;\hat{\boldsymbol{\beta}}_{\mathcal{T}}) = g'(t = s_{\mathcal{T}}(t_p+\tau;\psi_1,\psi_2);\hat{\boldsymbol{\beta}}_{\mathcal{C}}). \tag{5b}$$

The first constraint ensures that the pre-policy peak of daily deaths of the scaled (smoothed) epidemic in region $\mathcal{T}$ corresponds to the pre-policy peak in region $\mathcal{C}$. The second constraint ensures that the (smoothed) epidemics at the stage of the effective policy date in $\mathcal{T}$ are the same. Note that the first constraint uses the supremum of $g'(\cdot)$, as it is possible that the maximum is not on the interval—this is the case if the flow of deaths peaks after the effective policy date. If in at least one of the two regions the policy is effective only after the peak (see panel (a) of Figure 2), then $\arg\sup g'(t;\cdot) < t_p + \tau$, and there are two constraints (5a) and (5b) to the minimization problem. Otherwise, i.e., if both regions are before their peaks (as in panel (b)), the two constraints collapse to one, because the supremum is reached at the policy date.

Applied to the whole time series, the estimated parameters $\hat{\boldsymbol{\psi}}$ give a normalized version of the epidemic in region $\mathcal{T}$. To guide intuition, we continue to look at smooth representations of the epidemics. Consider first the illustrative scenario where the effective policy date is after the peak of the epidemic: the estimated parameter $\hat{\psi}_0$ scales up the epidemic in $\mathcal{T}$ such that the *magnitude* of the epidemic is the same as in region $\mathcal{C}$, as visualized in panel (c) of Figure 2. In panel (d), we show the adjustment in the alternative scenario, where the effective policy date is before the peak: the overall magnitude of the normalized epidemic remains lower than in region $\mathcal{C}$, reflecting that the policy affects the peak of the flow of deaths. In the last two panels (e) and

[8]Note that there is no "natural choice" for which region is the benchmark. Choosing $\mathcal{T}$ as benchmark region gives identical results for the policy effect.

Figure 3: Identification of Policy Effect: An Illustration

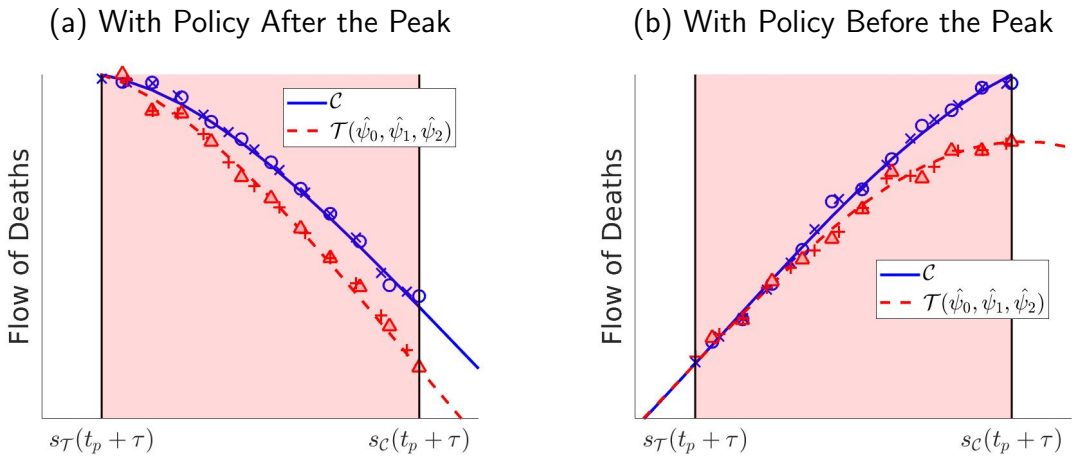

Notes: The figure zooms in on the overlap interval in panel (f) of Figure 2. It shows the GLF for $\mathcal{C}$, the adjusted GLF for $\mathcal{T}$, together with the data for $\mathcal{C}$ and the adjusted (normalized) data for $\mathcal{T}$.

(f) we move to stages s as opposed to time t on the x-axis. For region $\mathcal{C}$ nothing changes, and we still show the same epidemic as before. For region $\mathcal{T}$, we plot the epidemic adjusted for *time* and *speed* (and as before, for *magnitude*). To see this last step, note that the estimated parameters $\hat{\psi}_1$ and $\hat{\psi}_2$ assign a stage $s_{\mathcal{T}}(t; \hat{\psi}_1, \hat{\psi}_2)$ to every date t according to Equation (3). Accordingly, $t_{\mathcal{T}}(s; \cdot) = s_{\mathcal{T}}^{-1}(s; \cdot)$ gives the date t corresponding to a stage, and thus gives the adjusted flow of death at stage s as $\hat{\psi}_0 g'(t = t_{\mathcal{T}}(s; \cdot) = s_{\mathcal{T}}^{-1}(s; \cdot), \hat{\boldsymbol{\beta}}_{\mathcal{T}})$. With this, the stage is set to estimate the policy effect, to which we turn next.

Estimation of Policy Effect. If the epidemic in region $\mathcal{C}$ leads the one in region $\mathcal{T}$, then there is an interval D in terms of stages during which the policy is already implemented in $\mathcal{T}$, but not yet in $\mathcal{C}$, even though the policy is implemented at the same calendar date:

$$D = [s_{\mathcal{T}}(t_p + \tau; \hat{\psi}_1, \hat{\psi}_2), \ldots, s_{\mathcal{C}}(t_p + \tau)].$$

We refer to D as the overlap interval, and show it in panels (e) and (f) of Figure 2. In Figure 3 we zoom in on that overlap interval and again plot the smooth representations of the epidemic, $g'(\cdot)$. In the rest of the discussion, we focus on the scenario where the effective policy date is before the peaks of both regions (i.e., panel (b) of Figure 3), but everything goes through for other scenarios including the case in which the policy is introduced after the peaks of both regions (i.e., panel (a) of Figure 3).

For the estimation of the policy effect we do not rely on smoothed data, and instead directly apply the estimated normalization parameters to the observed data in the obtained overlap in-

terval. However, in order to do so, we first need to translate the overlap interval into discrete steps—as the flow of deaths is observed on discrete calendar dates t. Thus, consider

$$\begin{aligned}\bar{D} &= \{cl(s_{\mathcal{C}}(\min\{D\})), \ldots, fl(s_{\mathcal{C}}(\max\{D\}))\} \\ &= \{cl(s_{\mathcal{T}}(t_p+\tau;\hat{\psi}_1,\hat{\psi}_2)), \ldots, t_p+\tau\}\end{aligned} \tag{6}$$

where $fl(\cdot)$ and $cl(\cdot)$ denote the integer floor or integer ceiling, respectively. Note that the time t assigned to a stage $s \in \bar{D}$ for region $\mathcal{T}$ according to $t_{\mathcal{T}}(s) = s_{\mathcal{T}}^{-1}(s;\hat{\psi}_1,\hat{\psi}_2)$ is not discrete. Thus, we interpolate between $\hat{\psi}_0 y_{t=fl(t_{\mathcal{T}}(s)),\mathcal{T}}$ and $\hat{\psi}_0 y_{t=cl(t_{\mathcal{T}}(s)),\mathcal{T}}$ to obtain $\hat{\psi}_0 \hat{y}_{t=t_{\mathcal{T}}(s)),\mathcal{T}}$. The markers in Figure 3 show the obtained (scaled) data on the overlap interval: blue circles correspond to region $\mathcal{C}$ and red triangles show the corresponding flow of deaths for region $\mathcal{T}$. The distance function (1) to be minimized becomes

$$\|\ln(\hat{\psi}_0 \hat{y}_{t=t_{\mathcal{T}}(s)=s_{\mathcal{T}}^{-1}(s;\hat{\psi}_1,\hat{\psi}_2),\mathcal{T}}) - \ln(y_{t=s,\mathcal{C}}) - \ln(1+w(s;\gamma^p))\|_{s\in\bar{D}}. \tag{7}$$

In order to treat the data observations for both regions symmetrically, we also consider the following alternative representation of the interval D, which gives discrete dates for the normalized region $\mathcal{T}$:

$$\begin{aligned}\tilde{D} &= \{cl(s_{\mathcal{T}}^{-1}(\min\{D\};\hat{\psi}_1,\hat{\psi}_2)), \ldots, fl(s_{\mathcal{T}}^{-1}(\max\{D\};\hat{\psi}_1,\hat{\psi}_2))\} \\ &= \{t_p+\tau, \ldots, fl(s_{\mathcal{T}}^{-1}(t_p+\tau;\hat{\psi}_1,\hat{\psi}_2))\}.\end{aligned} \tag{8}$$

For all $\tilde{t} \in \tilde{D}$, for region $\mathcal{T}$, the raw data scaled to the epidemic magnitude of region $\mathcal{C}$ are observed on $t = \tilde{t}$: $\hat{\psi}_0 \cdot y_{t=\tilde{t},\mathcal{T}}$. In the same fashion as above, we now obtain $s(\tilde{t}) = s_{\mathcal{T}}(\tilde{t};\hat{\psi}_1,\hat{\psi}_2)$. We then interpolate between $y_{t=s=fl(s(\tilde{t})),\mathcal{C}}$ and $y_{t=s=cl(s(\tilde{t})),\mathcal{C}}$ to obtain $\hat{y}_{t=s=s_{\mathcal{T}}(\tilde{t};\hat{\psi}_1,\hat{\psi}_2),\mathcal{C}}$. The crosses in Figure 3 show the corresponding data: again in blue and red for regions $\mathcal{C}$ and $\mathcal{T}$, respectively. The distance function (1) to be minimized then becomes

$$\|\ln(\hat{\psi}_0 y_{t=\tilde{t},\mathcal{T}}) - \ln(\hat{y}_{t=s=s_{\mathcal{T}}(\tilde{t};\hat{\psi}_1,\hat{\psi}_2),\mathcal{C}}) - \ln(1+w(s=s_{\mathcal{T}}(\tilde{t};\hat{\psi}_1,\hat{\psi}_2);\gamma^p))\|_{\tilde{t}\in\tilde{D}} \tag{9}$$

We then stack (7) and (9) and minimize over γ_p, which gives our estimate of the policy effect in region $\mathcal{T}$.

3 Epidemic Dynamics and Policy Timeline in Spain

We now first describe the dynamic behavior of the Covid-19 epidemic in Spain focusing on the time path of the flow of deaths, and the associated stock—the cumulative number—of deaths. Then, we describe the timeline of the stay-home policy implementation in Spain.

The Epidemic Dynamics. Covid-19 was introduced in Spain through multiple routes (Díez-Fuertes et al., 2020). The first confirmed case of Covid-19 dates to January 31, 2020.[9] A sequence of cases largely related to individuals returning from trips to Lombardy, Italy, rapidly emerged throughout February. At that point, the country witnessed the diffusion of Covid-19 through several community clusters and, by March 13, cases had been confirmed in all of the fifty provinces in the country. Deaths followed infections with some lags. The first Covid-19 death occurred on Feb 13 in Valencia, although it was not until March 3 that the death was linked to Covid-19 in an autopsy.[10] We show the entire path of the daily flow of deaths and its associated stock for nationwide Spain and some sub-regions in Figure 4.

The nationwide flow of Covid-19 deaths rapidly increased from early to late March, with a number of daily Covid-19 deaths of 2 on March 1 to 870 on March 31—i.e., an increase from 0.042 to 18.50 daily deaths per one million inhabitants; see panel (a1) of Figure 4. The rapid increase in the flow of deaths is followed, after reaching its peak, by a slower pace decline; the number of daily deaths declines from March 31 to April 30 to 206—or to 4.38 per one million inhabitants. That is, as a function of time, the flow of deaths exhibits an asymmetric bell shape with a thicker tail to the right of the peak, i.e., right skewness. Further, directly associated with the behavior of the flow of deaths is that of the stock of deaths. The time path of the stock of deaths is S-shaped—a sigmoid; see panel (a2) of Figure 4. Then, note the asymmetry in flow of deaths goes hand in hand with an analogous asymmetry in the stock of deaths. For example, the accumulated number of Covid-19 deaths that occur during March—i.e. during the thirty days that precede the peak of the epidemic—is 10,050 whereas the total number of deaths that occur during April—i.e., during the thirty days that follow the peak of the epidemic—is 15,970, which speaks to the right skewness of the flow of deaths. As of July 31st, the cumulative number of deaths kept increasing with a total amount of 28,279 deaths in stock.

Within Spain, we distinguish the behavior of the epidemic in the region of Madrid and the rest of Spain: an artificial region that consists of Spain without the region of Madrid. In Madrid, the number of daily Covid-19 deaths reaches a maximum of 327 in March 27, whereas for the rest of Spain this figure is 655 in March 30. That is, the epidemic reaches its peak earlier in Madrid than in the rest of Spain. In per capita terms, the peak is also of larger magnitude in Madrid than in the rest of Spain. Madrid reaches a maximum of 49.23 deaths per one million inhabitants,

[9] A German tourist tested positive in La Gomera, Canary Islands.

[10] It is then when distance measures are publicly spoken of by the government for the first time, although not enforced by any means. Indeed, official La Liga soccer games with average attendance of more than 20,000 are played during the weekend of March 7 and 8 throughout the country, and massive demonstrations are held for Women's Day on March 8. During the following week some country- and regional-level officials emphasized the need to take into account simple but what at that time were understood as key measures such as washing hands frequently, covering one's mouth and nose when sneezing with tissues, handkerchiefs, or forearms, avoiding sharing objects in meetings. Those who show symptoms are also asked to voluntarily stay home.

Figure 4: Covid-19 Deaths in Spain

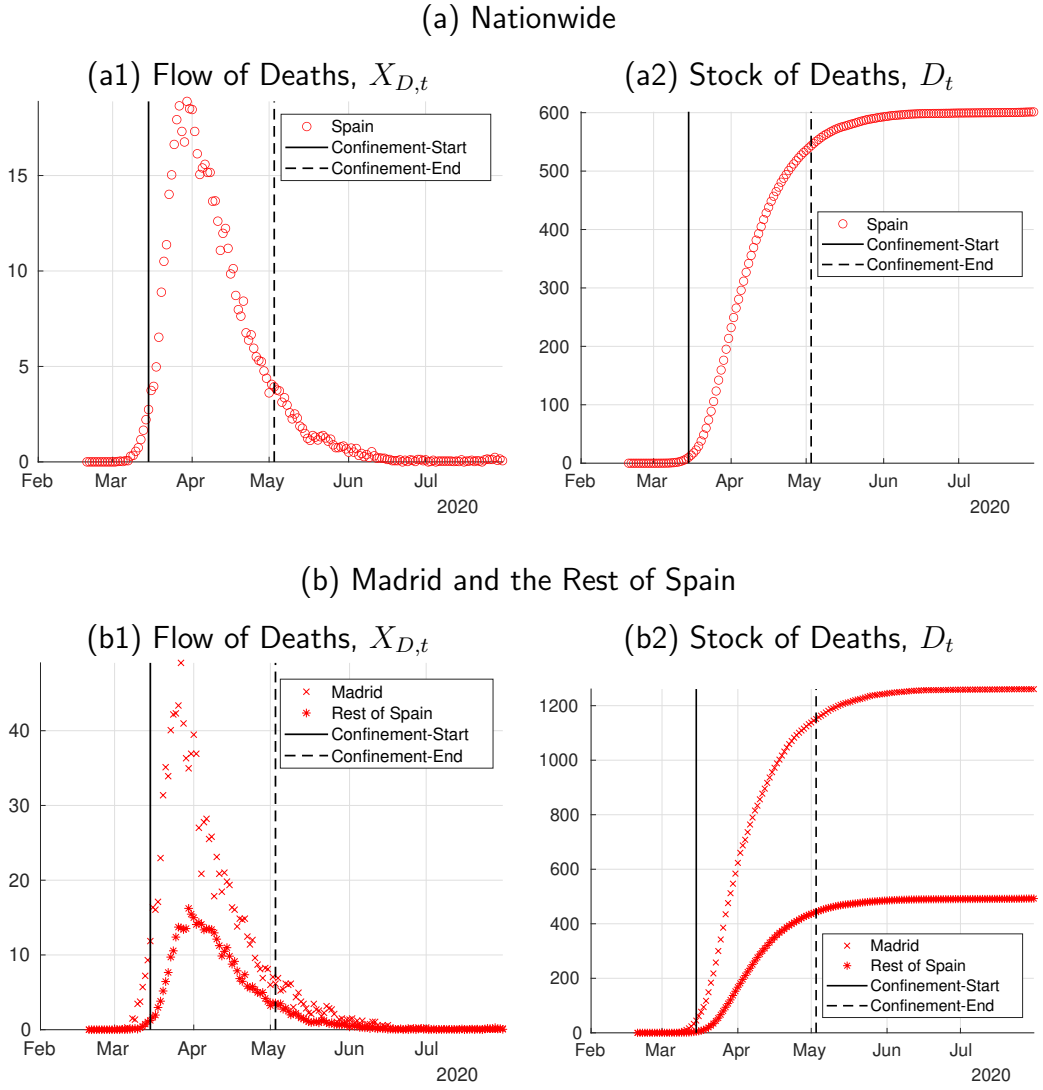

Notes: Panel (a) shows the flow of detahs (a1) and stock of deaths (a2) associated with Covid-19 in Spain. In panel (b) we separately reproduce these results for the autonomous community of Madrid and the rest of Spain—i.e. an artificial region that consists of Spain without Madrid. All panels are expressed per million inhabitants of each region, with Spain having 47 million inhabitants and Madrid 6.6 million. *Source of data:* Instituto de Salud Carlos III.

whereas for the rest of Spain this figure is 16.22; see panel (b1) of Figure 4. Further, in Madrid, the accumulated number of deaths is 2,897 during the thirty days before the peak of the epidemic whereas this figure is 4,488 during the following thirty days. These numbers are, respectively, 4,846 and 12,475, for the rest of Spain, which suggests a larger asymmetry—right-skewness—in the rest of Spain than in Madrid. This is confirmed with a positive skewness statistic for each of

the two regions that is larger for the rest of Spain than for Madrid.[11]

In order to describe the epidemic dynamics we focus on the flow of deaths. We use the data on Covid-19 deaths provided by the Ministerio de Sanidad in Spain.[12] The criteria imposed by the Ministerio in order to homogenize the death data separately collected by each region—or autonomous community—is to define as Covid-19 deaths those that were tested positive for Covid-19 using PCR tests. While the measurement of Covid-19 deaths is not free of problems—including potential measurement error from PCR testing, we regard the flow of deaths as a more accurate measure compared to official number of new infections (or cases). Our rationale to characterize the epidemic using deaths—as opposed to infections or other margins of the epidemic—is the notorious lack of nationally representative serological testing throughout the course of the epidemic which implies that the actual dynamics of the infected population that would be required to conduct our analysis—if we were to focus on infections—is simply unknown. There are limited exceptions to this. Notably, in the case of Spain, a nationally representative serological study is currently ongoing. Unfortunately, this study was initiated on April 27, that is, approximately 1.5 months after the stay-home policy was enacted and when the studied wave of the epidemic was already starting to flat out—e.g. at the time the nationally representative testing was conducted the flow of deaths was already below 5.5 per million inhabitants.[13] Altogether, the official measure of the infected population at a given point in time is subject to large measurement error that potentially depends not only on the growing availability and quality of PCR tests but also on the selection of individuals that are tested (i.e., those that show symptoms and seek for medical help). In addition, it can be shown that the entire epidemic dynamics—including new infections, recoveries and active infections—can be recovered using the observed number of deaths by imposing some assumptions on the arrival process of deaths, see Appendix A.

Stay-Home Policy Timeline. On March 14, the President of Spain, Pedro Sánchez, declared a nationwide State of Alarm, which was enacted on March 15 for an initial duration of 14 days.By this ruling, all residents were mandated to remain in their habitual residence at all times except to buy food, purchase medicines and attend work or emergencies. This stay-home policy came together with a set of economic lockdown restrictions that temporarily closed non-essential shops and businesses, including bars, restaurants, cafes, cinemas, commercial and retail businesses, etc. On March 22, shortly after exceeding 1,000 deaths, the government announced the petition to extend the State of Alarm in the nation until April 11, which the Congress ratified on March 28. On March 29, the Spanish government further banned all non-essential economic activities

[11] The skewness coefficients for Spain, Madrid, and the rest of Spain are 1.03, 0.74, and 1.05 respectively.

[12] The data from the Ministerio de Sanidad can be found under the following link: www.mscbs.gob.es

[13] The Spanish nationally representative serological study consists of several unbalanced waves across time and space with, arguably, a too small sample size within regions; see Pollan et al. (2020).

between March 29 and April 11. Starting April 13 some restrictions were lifted: non-essential workers for whom telework was not feasible were allowed to return to work (e.g. in construction).[14] The government began the distribution of millions of face masks in public transportation hubs. On April 21, the government announced that from April 27 on children under the age of 14 were able to go out on short walks with their parents or other adults living in the same household.

The stay-home policy ended on May 2. On April 28, the government announced a plan for easing lockdown restrictions. The plan has four phases, numbered 0 through 3. Phase 0 allowed people out of their homes for short walks and individual sports from May 2. The transition across phases could differ by province according to public health indicators such as the number of Covid-19 cases and the capacity of the healthcare system. The state of alarm expired at midnight of Sunday June 21, and Spain entered a phase referred to as "new normality" in which the control of policy restrictions was fully decentralized and passed to the hands of each autonomous community.

4 Lives Saved by the Stay-Home Policy in Spain

4.1 Smooth Epidemic Dynamics

The first step of the application of our method is to fit smooth functions to the (regional) epidemics on which the normalization is based. We use a generalized logistic function (GLF), which is able to capture salient features of the observed epidemic dynamics: an asymmetric bell-shaped time path of the flow of deaths (normalized by population size), and the implied S-shaped time path of the stock of deaths (normalized by population size).[15]

The stock of deaths is given as

$$g(t;\boldsymbol{\beta}) = \frac{\beta_0}{\left[1+\beta_3 \exp\left[-\beta_1\left(t-\beta_2\right)\right]\right]^{\frac{1}{\beta_3}}}, \tag{10}$$

with $\boldsymbol{\beta} = \{\beta_0, \beta_1, \beta_2, \beta_3\}$, and the flow of deaths follows as the first analytical derivative of (10) with respect to time, giving

$$g'(t;\boldsymbol{\beta}) = \frac{\partial g(t;\boldsymbol{\beta})}{\partial t} = \beta_1 \cdot g(t;\boldsymbol{\beta}) \cdot \frac{1}{\beta_3 + \exp\left[\beta_1\left(t-\beta_2\right)\right]}. \tag{11}$$

[14] The Ministerio de Sanidad elaborated a guide for good practice at work that included, among others, the use of masks (in case workers interacted with other individuals), the use of bulkheads or shields (e.g., in offices, restaurants and retail cashiers), an encouragement for the use of credit cards as method of payment, a recommended temperature of twenty-three to twenty-six degrees Celsius at the place of work, and the washing of uniforms on a daily basis at higher than sixty degrees Celsius. In addition, the Minister of Health, Salvador Illa, emphasized the importance of keeping physical distance and of frequent washing hands.

[15] The generalized logistic function—also referred to as Richards growth curve—is also employed by Lee et al. (2020) for modelling Covid-19 infection trajectories. We are currently exploring alternative smooth functions to track the epidemic.

Figure 5: Normalization of the Epidemic: By Regions

(a) Before Normalization

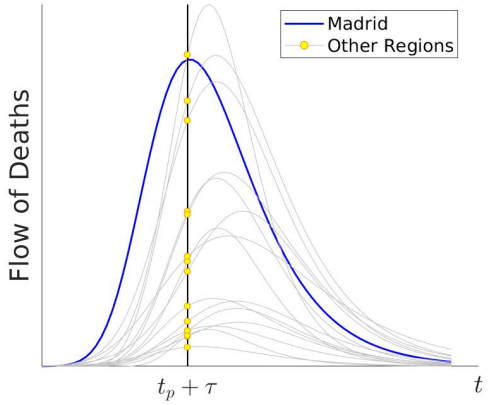

(b) After Normalization

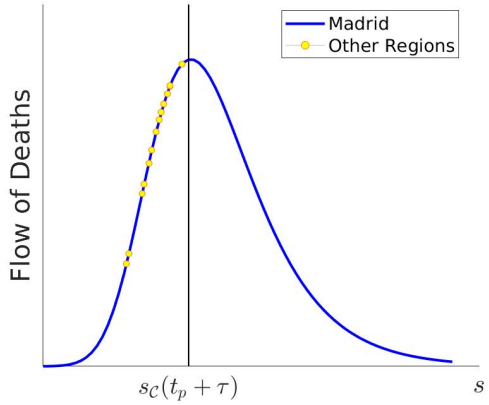

Notes: Panel (a) shows the time path of the flow of deaths—as a function of calendar time t—for each region in Spain. Panel (b) shows the *stages* s—at the effective policy date for the various regions after applying our normalization procedure described in Section 2.

Thus, β_0 is the maximum value of the stock of deaths for $t \to \infty$, β_1 is the average logistic growth rate of the stock of deaths, β_2 is the inflection point in the time path of the stock of deaths (the maximum of the flow), and $\beta_3 > 0$ measures the degree of asymmetry in the time path of the stock of deaths (right skewness in the time path of the flow).[16]

We fit $g'(\cdot)$ to data starting on February 20, 2020[17], which in our notation is equal to $t = 1$. Period $t_0(r)$ is the region specific start period in the estimation, which we determine as the period in which we observe the first death in the respective region giving $t_S^0 = 13$, $t_M^0 = 13$ and $t_R^0 = 14$.[18] Our sample is restricted to be of length $T(\tau)$, which is indexed by τ, the lag parameter at which the policy becomes effective. To determine $T(\tau)$ we take the date of the end of the studied policy intervention (i.e., the lifting of the strict confinement measures), which is May 2, 2020, period t_e, and add the policy lag parameter, thus $T(\tau) = t_e + \tau$, reflecting the assumption that the flow of deaths is affected by the policy change with time lag τ. Finally, we conduct statistical inference by bootstrapping confidence bands. It is crucial for our normalization that $g'(\cdot)$ matches the flow of death time series before the effective policy date $t_p+\tau$ well. Figure 6

[16] Note that if $\beta_3 = 1$, then the function (10) is the logistic function, and for β_3 approaching 0 from the side of positive real numbers it approaches the Gompertz growth law.

[17] We thereby exclude one outlier in the data on the flow of death. As described in Section 3 a first death is reported in Valencia on February 13 followed by zero death reports in all regions until the second death report in Madrid on March 3, 2020.

[18] We clean (very few) observations with zero death reports within the sample period $t_r^0, \ldots, T(\tau)$ by linear interpolation.

Figure 6: Normalization of the Epidemics: Madrid ($\mathcal{C}$) vs. Rest of Spain ($\mathcal{T}$)

(a) Before Normalization

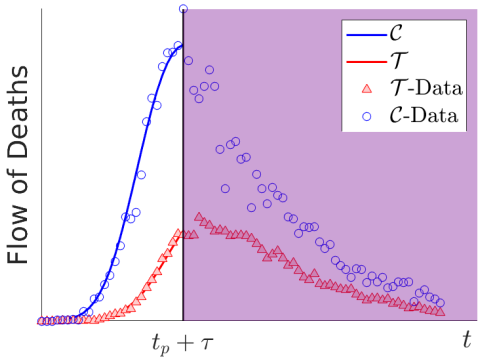

(b) After Normalization

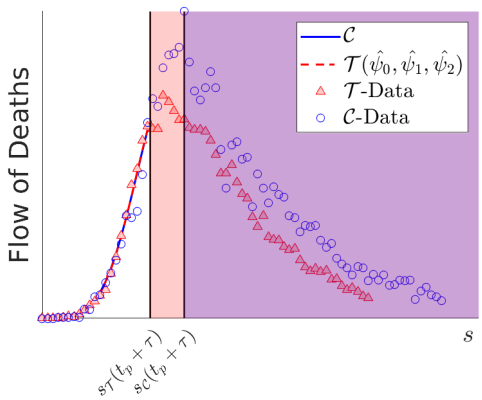

Notes: Panel (a) shows the epidemics in Madrid ($\mathcal{C}$) and the rest of Spain ($\mathcal{T}$)), panel (b) shows the normalized epidemics. The fitted lines for $t < t_p + \tau$ show the smooth epidemics pre-policy that are used in the normalization procedure.

shows that this is the case for our benchmark choice of $\tau = 12$. Appendix B summarizes the parameter estimates of the GLF and provides details on our bootstrapping procedure.

4.2 Estimates of Lives Saved

Effect During Overlap Interval. In panel (a) of Figure 5, we show the epidemic path in terms of Covid-19 deaths per one million inhabitants separately for Spanish regions. The region of Madrid (blue line) shows an epidemic path that precedes all other regions with an earlier rise, peak and decline than the rest of regions in calendar time.[19] Further, normalizing the pre-policy epidemic path of all regions to Madrid as described in Section 2, we find that at the time of policy implementation the region of Madrid is at the latest *stage* of the epidemic across all regions, see panel (b) of Figure 5. Since the epidemic in Madrid thus leads the other regions it constitutes a suitable candidate as control region $\mathcal{C} = M$ for our analysis.

Next, we create a treatment region $\mathcal{T}$ formed by the rest of Spanish regions—i.e., an artificial region that consists of Spain without Madrid, thus $\mathcal{T} = R$, where R stands in for Rest of Spain. We show the epidemic paths of the regions Madrid and the rest of Spain before and after normalization, respectively, in panels (a) and (b) of Figure 6. Before normalization, we find that the epidemic in Madrid starts earlier, evolves faster, and has a larger magnitude than the rest of Spain. After normalization, Madrid and the rest of Spain follow the same pre-policy epidemic path. Notice that the normalization is under an effect of policy that occurs at date $t_p + \tau$, where

[19] Madrid is the region with the second largest peak, 49.23 deaths per million inhabitants, following a peak of 55.02 deaths per million inhabitants in Castilla y León and preceding a peak of 38.62 deaths per million inhabitants in Castilla La Mancha.

Figure 7: Effects of Stay-Home Policy: Madrid ($\mathcal{C}$) vs. Rest of Spain ($\mathcal{T}$)

(a) Overlap Interval

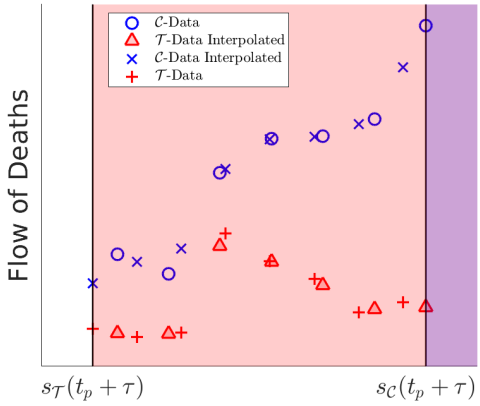

(b) Estimated Effect with Different Lags, τ

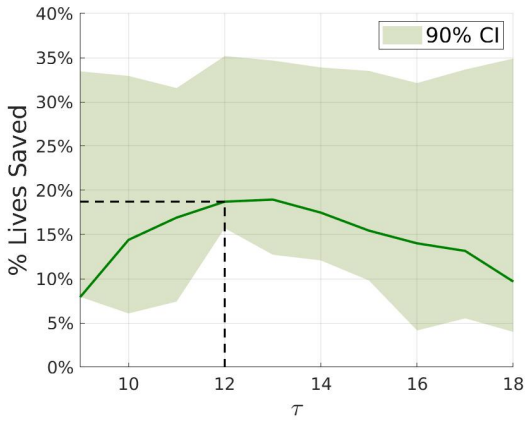

Notes: Panel (a) shows the epidemic path of control group, Madrid $\mathcal{C}$, and the normalized epidemic path of our treatment group, the rest of Spain $\mathcal{T}$ within the overlap interval $D(s)$. Panel (b) shows the effects of policy in terms of percentage of lives saved as a function of τ.

we use a benchmark policy lag of τ equal to twelve days, on which we conduct robustness below.

The normalization unveils an overlap interval in terms of *stages*, in which the region of Madrid is not yet under the effect of policy whereas the rest of Spain is, i.e., the interval $D_R = [s_R(t_p+\tau), s_M(t_p+\tau)]$, cf. Section 2. The overlap interval is seven days long. We compute the average effect of policy as the average difference between the deaths in Madrid and the normalized rest of Spain within the overlap interval applying the methods described in Section 2. Panel (a) of Figure 7 shows the normalized data on the overlap interval, where the normalized rest of Spain faces the stay-home policy while the region of Madrid does not. The distance between the time path of the flow of deaths in Madrid and the time path in the normalized rest of Spain measures the effects of policy understood as the amount of lives saved.

As distance function $\omega(t;\gamma)$ we choose a simple dummy variable assuming an effect on lives saved from period $t_p+\tau+1$ onwards

$$\omega(t;\gamma_R^p) = \begin{cases} 0 & \text{for } t = t_p+\tau \\ -\gamma_R^p & \text{for } t > t_p+\tau, \end{cases} \tag{12}$$

and thus our estimate $\hat{\gamma}_R^p$ captures the average reduction of deaths in the overlap interval. We next translate this estimate into the number and the percent of lives saved. We denote by y_{tR} the number of deaths in the rest of Spain for any time period $t = \tilde{t} \in \tilde{D}_R = \{t_p+\tau, \ldots, fl(s_R^{-1}(t_p+\tau)\}$. Remember from equation (8) in Section 2 that $\tilde{D}_R$ is the time interval which assigns the

Table 1: Effect of Stay-Home Policy: Madrid ($\mathcal{C}$) vs. Rest of Spain ($\mathcal{T}$)

	Overlap (1)	Post-Overlap (2)	Overall (3)
% Lives Saved:	18.7	19.6	19.4
	[15.7;35.1]	[16.3;36.9]	[16.1;36.5]
# Lives Saved:	1,074	2,712	3,787
	[888;2,028]	[2,311;6,935]	[3,248;8,953]
# Days of Overlap:	7	-	-

Notes: Estimates of number and percent of lives saved from they stay-home policy for a policy lag of $\tau = 12$ days. Table shows the Bootstrapped 90% confidence bounds in parenthesis.

calendar time of the epidemic in the treatment region to the stages of the overlap interval D_R. In the calculations that follow we base the number of lives saved on the observed flow of death in the treatment region, and thus we refer explicitly to the interval on which data is observed. Then, the counterfactual number of deaths in period t, region R follows from equation (1) as $\frac{1}{1+\omega(t,\hat{\gamma}_R^p)} y_{tR}$ so that the number of lives saved is

$$\hat{l}_{tR} = -\frac{\omega(t,\hat{\gamma}_R^p)}{1+\omega(t,\hat{\gamma}_R^p)} y_{tR}.$$

The estimated total number of lives saved $\hat{L}_R^{\tilde{D}_R}$ and the corresponding total number of deaths $Y_R^{\tilde{D}_R}$ is thus

$$\hat{L}_R^{\tilde{D}_R} = \sum_{t=t_p+\tau}^{fl(s_R^{-1}(t_p+\tau))} \hat{l}_{tR}, \qquad Y_R^{\tilde{D}_R} = \sum_{t=t_p+\tau}^{fl(s_R^{-1}(t_p+\tau))} y_{tR}.$$

Consequently, the percentage of lives saved in each period on time interval $\tilde{D}_R$, which relates the total number of lives saved to the counterfactual deaths on that interval, is

$$\frac{\hat{L}_R^{\tilde{D}_R}}{\hat{L}_R^{\tilde{D}_R} + Y_R^{\tilde{D}_R}}.$$

Our estimate of the percentage of lives saved due to implementing the policy in the rest of Spain according to this definition is 18.7%, see column (1) in Table 1. This estimate is significantly different from zero. The corresponding number of lives saved $L_R^{\tilde{D}_R}$ is about 1,074.

Role of the Time Lag Until Effectiveness. Our baseline results relate to a policy lag parameter of τ equal to twelve. We now investigate the robustness of our main result with respect to this lag parameter. In panel (b) of Figure 7 we plot the effects of the stay-home policy, i.e., the percentage of lives saved by the policy on the overlap interval, as function of the lag parameter τ, which displays a clear inverse u-shaped pattern. First, the percentage of lives saved monotonically increases with τ starting from $\tau = 9$ with a point estimate of the percentage of lives saved of 7.9%. This effect increases until $\tau = 13$, where we reach a maximum effect of a percentage of 18.9% of lives saved, with a corresponding total number of lives saved of $1,096$ very close to our main estimates for $\tau = 12$. The effects of the stay-home policy decrease afterwards. Indeed, the percentage of lives saved become not significantly different from zero for lags larger than τ equal to eighteen.

Extrapolation to End of Stay-Home Policy. Based on our estimates for $\tau = 12$ we further calculate the implied number of lives saved after the overlap interval by extrapolating the policy effect. To this end, we assume that the policy parameter estimate $\hat{\gamma}_p^R$ is the same as the one estimated on the overlap interval for all periods after the overlap, i.e., for the treatment region, we use the data observed for all $t = \tilde{t} \in \{fl(s_R^{-1}(t_p + \tau)) + 1, \ldots, T(\tau)\}$. Table 1 separately shows the results for the post-overlap interval and the overall effects in, respectively, columns (2) and (3). We compute the number of lives saved each period as $\hat{l}_{tR} = -\frac{\omega(t,\hat{\gamma}_R^p)}{1+\omega(t,\hat{\gamma}_R^p)} y_{tR}$, the total number of lives saved as $\hat{L}_R = \sum_{t=fl(s_R^{-1}(t_p+\tau))+1}^{T(\tau)} \hat{l}_{tR}$, the total number of deaths on this time interval as $Y_R = \sum_{t=fl(s_R^{-1}(t_p+\tau))+1}^{T(\tau)} y_{tR}$, and, finally, the percentage of lives saved as $\frac{\hat{L}_R}{\hat{L}_R+Y_R}$. According to our estimate, from the date of confinement until May 2 when the first wave of the epidemic ends—i.e. the flow of deaths flattens out—and the strict measures were lifted about 19.4% of lives—or 3,787 lives—were saved in Spain without Madrid.

Below we will further extrapolate our estimates to the whole of Spain. To this purpose we need an estimate of the number of lives saved in the control region, Madrid. We will base this estimate on an extrapolation of the extent of policy effectiveness by epidemic stages at the time of policy implementation to which we turn next.

Effectiveness of Policy Over the Course of the Epidemic. How do the effects of the stay-home policy differ by the *stage* of the epidemic? To address this question we exploit the heterogeneity in the *stage* of the epidemic across regions at the time of policy implementation as documented above in Figure 5. We split the regions in our benchmark treatment group—i.e., Spain without Madrid—into three subgroups according to the region-specific *stage* at which the nationwide policy was implemented. We label the first, second and last of these subgroups respectively as early, mid and late stage implementers of the stay-home policy. The treatment subgroup with early stage implementers of the policy consists of Aragon, Baleares, Cantabria and

Table 2: Effects of Stay-Home Policy: By Stage of Policy Implementation

(a) Early Stage Implementers:

	Overlap	Post-Overlap	Overall
% Lives Saved:	33.2	33.5	33.3
	[27.9;42.8]	[28.1;43.22]	[28.0;42.9]
# Lives Saved:	432	199	631
	[354;549]	[168;333]	[518;877]
# Days of Overlap:	11	-	-

(b) Mid Stage Implementers:

	Overlap	Post-Overlap	Overall
% Lives Saved:	24.1	25.1	24.8
	[18.5;38.8]	[19.3;40.4]	[19.1;40.1]
# Lives Saved:	1,266	2,725	3,991
	[978;2,082]	[2,178;6,051]	[3,149;8,104]
# Days of Overlap:	7	-	-

(c) Last Stage Implementers:

	Overlap	Post-Overlap	Overall
% Lives Saved:	8.2	9.5	9.3
	[2.6;32.4]	[2.9;35.9]	[2.8;35.5]
# Lives Saved:	33	214	248
	[10;127]	[61;1,142]	[71;1,270]
# Days of Overlap:	4	-	-

Notes: These estimates refer are associated with a lagged effect of $\tau = 12$ Days. Table shows the Bootstrapped 90% confidence bounds in parenthesis.

Murcia, and is associated with a overlap interval of eleven days. The treatment subgroup with late implementers consists of Andalucia, Canary Islands and Valencia, and is associated with an overlap interval of four days. The rest of Spanish regions, excluding Madrid, fall into the group that implements the policy at some mid stages with an overlap interval of seven days long.

We find that regions on which the stay-home policy is implemented in earlier *stages* of the

epidemic benefit the most in terms of the percentage of lives saved. For early implementers, the stay-home policy saves on average 33.2% of lives on the overlap interval. For the mid-stage implementers, the stay-home policy saves 24.1% of lives. For late implementers, the stay-home policy saves 8.2% of lives. That is, the effectiveness of policy for the early implementers is significantly larger—by a factor of four—than that for the late implementers. Our results also imply a rapid drop in policy effectiveness since, in terms of stages, the early implementers enter policy approximately one week earlier than the late implementers. That is, the effectiveness of policy drops by approximately three fourths in a matter of just one week. Extending the estimation after the overlap interval delivers similar insights, see Table 2.

We further unpack the effects of policy by region. For example, as part of the subgroup of regions that implemented the policy earlier, Baleares, implemented the policy 11 days earlier—in terms of *stages*—than Madrid and shows an effect of percentage of lives saved by the policy of 46.9; the largest effect across Spanish regions. As part of the subgroup of regions that implemented the policy in mid stages of the epidemic, La Rioja, implemented the policy 5 days earlier—in terms of *stages*—than Madrid and shows an effect of percentage of lives saved by the policy of 26. Within the regions that implemented the policy at later stages, Valencia, that implemented the policy 3 days—in terms of stages—before the region of Madrid, saved 4.6 per cent of lives in the overlap interval. Figure 8 summarizes the effects of policy by region.

Our results imply that the effectiveness of policy relies on the stage of the epidemic at which the policy is implemented. In regions where the policy was implemented relatively early—in terms of stages—the policy caught the epidemic at a stage where it reduced the death toll by more than one-third. However, the effect of policy rapidly more than quartered for regions where the policy was implemented one week later.

Extrapolation to Spain. Finally, we extrapolate our estimates to compute the number of lives saved in Spain. To this purpose we first need an estimate for the lives saved in Madrid, the control region. We first regress the region specific estimates of the policy effects $\hat{\gamma}_r^p$ on the *stages* $s_r(t_p + \tau)$ at policy implementation in the respective regions[20] according to

$$\ln(\gamma_r) = \alpha_0 + \alpha_1 s_r + \epsilon_r. \tag{13}$$

We then use the result of the regression to predict the value of the policy effect in Madrid. Next, we apply this policy effect estimate to compute the number of lives saved in Madrid following the same steps outlined above, for all days after policy implementation $t = t_p + \tau + 1, \ldots, T(\tau)$. Summing up, our estimates imply 237 lives saved corresponding to 4.1% of the counterfactual

[20] The correlation between the policy effect parameters γ_r^p and the stages at policy implementation s_r is similar to the one between stages and percent lives saved shown Figure 8.

Figure 8: Effects of Stay-Home Policy: By Region

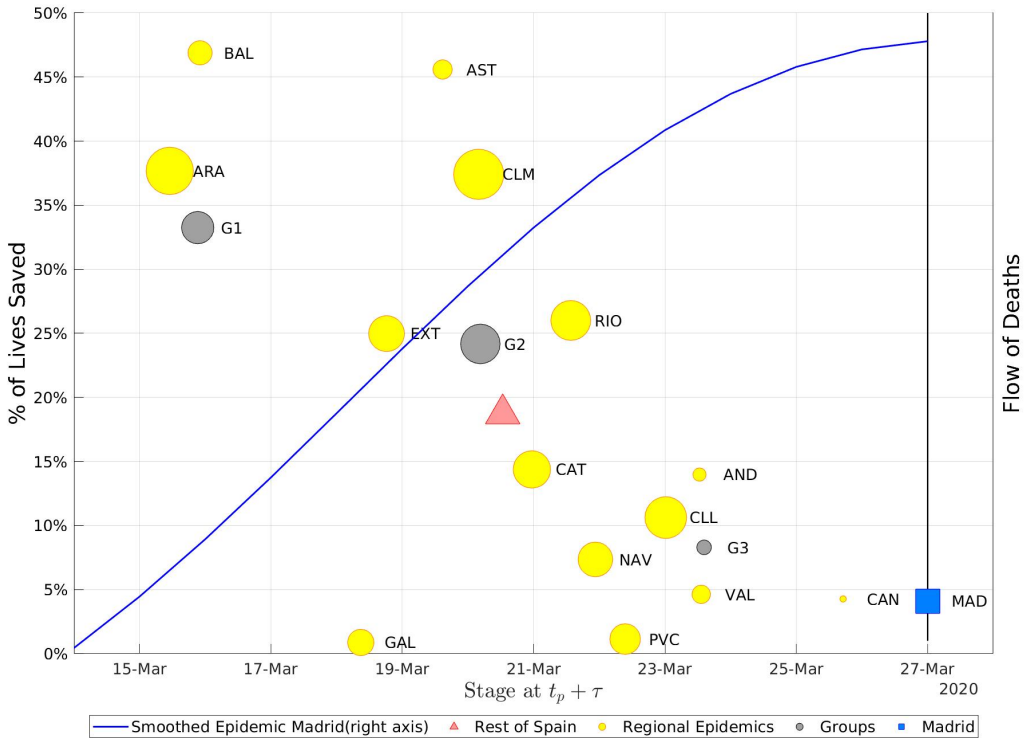

Notes: This figure shows the region-specific effects of policy against the epidemic *stage* of policy implementation by region. The effects of policy are defined by the percentage of lives saved in the overlap interval. The list of regions (yellow circles) is denoted by: Andalucia (AND), Aragon (ARA), Asturias (AST), Baleares (BAL), Canarias (CAN), Cantabria (CNT), Castilla-La Mancha (CLM), Castilla y Leon (CLL), Catalunya (CAT), Ceuta (CEU), Valencia (VAL), Extremadura (EXT), Galicia (GAL), Madrid (MAD), Melilla (MEL), Murcia (MUR), Navarra (NAV), Pais Vasco (PVC), La Rioja (RIO). We also plot the three subgroups (grey circles) in Table 2: Early-stage implementers (G1); Mid-stage implementers (G2); and Late-stage implementers (G3). The size of the yellow and grey circles is the stock of deaths per thousand inhabitants accumulated during the overlap period. The number shown for Madrid is computed using the extrapolated policy effect on the overall period; accordingly the size represents the accumulated stock of deaths per thousand inhabitants between $t_p + \tau + 1$ and $T(\tau)$.

deaths in Madrid. Finally, we add this to the number of lives saved in the rest of Spain, which gives a total number of lives saved of $4,024$.[21]

[21] An alternative estimate for Madrid, which takes into account the correlation between stage at policy effectiveness and percent of lives by groups of regions and not directly by regions, is to directly base the extrapolation for Madrid on our point estimate for the late implementers. We accordingly get a total number of lives saved in Madrid of 544 (or 9.02%), and thus a total number of lives saved in Spain of $4,331$.

To put these numbers into perspective, note that the total accumulated deaths at period $T(\tau)$ relative to one million of the population in Madrid is 5.7, whereas in the region rest of Spain it is 4.7. The ratio of these two numbers is 1.21, and thus the total death toll in Madrid exceeds the total death toll in the rest of Spain by about 21%. The corresponding ratio of lives saved is 0.06, thus lives saved in Madrid relative to the rest of Spain fall short by roughly 94%. This exemplifies the key effect of mid-stage versus late-stage implementation.

4.3 Estimating Effectiveness on Excess Mortality

Our benchmark measurement of Covid-19 deaths—defined as those tested positive for Covid-19 using PCR tests—may be mis-measured, because of lack of necessary testing equipment during the onset of the epidemic or unreliable accuracy of the PCR testing can affect the prevalence of Covid-19 deaths. Estimates of excess deaths—detrended and deseasonalized—are an alternative measure that also captures deaths that are indirectly happening due to Covid-19. On the one hand, ICUs at full capicity might limit access for non-Covid-19 patients and the lockdown policy may have triggered adverse reactions such that patients with other illnesses did not visit hospitals for reasons of fear. On the other hand, the deaths toll might have been reduced by fewer deaths from work- or traffic-related accidents that are not happening due to the stay-home policy implementation. All in all, the total reduction of excess deaths from the stay-home policy are a measure of interest by itself.

Table 3 reports our results for excess deaths for the region rest of Spain. As with the directly attributed Covid-19 deaths we find that the point estimates are inverse-u shaped in the policy lag parameter τ. In contrast to our previous findings reported in Table 1, confidence bands are large so that the estimates are insignificant.[22] Also, the peak of the policy effect for excess deaths is at $\tau = 16$ rather than $\tau = 12$. Otherwise, the point estimates in terms of the total number of lives saved are similar to those reported above for Covid-19 deaths and, according to the (insignificant) point estimate, the total number of lives saved in the region rest of Spain for the period since the lockdown became effective exceeds our previous estimate based on Covid-19 deaths; Table 1 reports 3845 deaths whereas the excess mortality data suggest a total number of lives saved of 4169. The difference is, of course, insignificant.

However, our results based on excess deaths data are still preliminary. The excess mortality data are computed relative to a base mortality, which we take as given from the predictions of the Instituto de Salud Carlos III (ISCIII) thus treating it as a black box. If systematic time variation in these estimates happens in the same time period when we measure the policy effect (in terms

[22]The reason for the higher confidence bands may be associated with additional noisiness introduced by the expected mortality. In our bootstrap procedure we do not take the statistical uncertainty of the expected death into account but directly bootstrap on the difference between observed deaths and expected deaths, which we take from the Instituto de Salud Carlos III.

Table 3: Effect of Stay-Home Policy on Total Lives Saved: Madrid ($\mathcal{C}$) vs. Rest of Spain ($\mathcal{T}$)

$\tau = 16$	Overlap (1)	Post-Overlap (2)	Overall (3)
% Lives Saved:	14.9	15.9	15.4
	[-29.3;21.8]	[-31.2;23.2]	[-30.3;22.6]
# Lives Saved:	1,521	2,224	3,745
	[-2,572;2,196]	[-3,022;3,824]	[-5,500;6,033]

Notes: Estimates of number and percent of lives saved according to the excess mortality data from they stay-home policy for a policy lag of $\tau = 16$ days. The bootstrapped 90% confidence bounds are reported in parenthesis.

of stages during the overlap interval) then this will bias our estimates.[23] For this reason we are currently seeking access to the ISCIII data on which the baseline estimates are based.

5 Conclusion

We develop a novel empirical approach to estimate the effectiveness of public policies against a pandemic. Our method consists of normalizing region-specific pre-policy epidemic dynamics to an exact same epidemic path. This approach uncovers heterogeneity across regions in the *stage* of the epidemic at the time of policy intervention. In particular, we find an interval—in terms of *stages*—in which the epidemic path of a control region unaffected by policy overlaps with a treatment region affected by policy. This overlap interval provides the basis for a clean identification of the effects of policy.

We apply our methodology to Spain, where we find that the regional epidemic in Madrid leads the ones in other Spanish regions and estimate that during an overlap interval of one week about 18.7% of lives were saved in the rest of Spain. There is considerable variation in this effect across disaggregated regions of Spain, and our estimates are larger for those regions that were at an earlier *stage* of the epidemic when the policy was implemented. Further, the effectiveness of policy rapidly declines across epidemic stages—dropping by three fourths in a matter of a week. Extrapolating the estimated policy effect to Madrid and until the policy was lifted, we find that the nationwide stay-home policy saved 15.9% of lives during the first wave of the pandemic.

In studies that quantify the trade-off between saving lives and losing economic activity the effectiveness of stay-home policies on the number of lives saved is a necessary input. Our estimates both in terms of the average effect as well as its variation across stages will provide useful information for calibrating these models.

[23] Estimates based on total mortality itself do not suffer from this problem, but are affected by seasonality.

References

Abadie, A., Diamond, A., and Hainmueller, J. (2010). Synthetic Control Methods for Comparative Case Studies: Estimating the Effect of California's Tobacco Control Program. Journal of the American Statistical Association, 105(490):493–505.

Abadie, A. and Gardeazabal, J. (2003). The Economic Costs of Conflict: A Case Study of the Basque Country. American Economic Review, 93(1):113–132.

Alvarez, F. E., Argente, D., and Lippi, F. (2020). A Simple Planning Problem for COVID-19 Lockdown. NBER Working Papers 26981, National Bureau of Economic Research, Inc.

Atkeson, A. (2020). What will be the economic impact of covid-19 in the us? rough estimates of disease scenarios. Working Paper 26867, National Bureau of Economic Research.

Barro, R. J., Ursúa, J. F., and Weng, J. (2020). The coronavirus and the great influenza pandemic: Lessons from the "spanish flu" for the coronavirus's potential effects on mortality and economic activity. Working Paper 26866, National Bureau of Economic Research.

Bootsma, M. C. J. and Ferguson, N. M. (2007). The effect of public health measures on the 1918 influenza pandemic in u.s. cities. Proceedings of the National Academy of Sciences, 104(18):7588–7593.

CDC (2014). Updated Preparedness and Response Framework for Influenza Pandemics. Centers for Disease Control and Prevention, Morbidity and Mortality Weekly Report, 63(6).

Cervellati, M. and Sunde, U. (2015). The economic and demographic transition, mortality, and comparative development. American Economic Journal: Macroeconomics, 7(3):189–225.

Dave, D. M., Friedson, A. I., Matsuzawa, K., and Sabia, J. J. (2020). When do shelter-in-place orders fight covid-19 best? policy heterogeneity across states and adoption time. Working Paper 27091, National Bureau of Economic Research.

Delventhal, M. J., Fernández-Villaverde, J., and Guner, N. (2019). Demographic transitions across time and space. Technical report.

Díez-Fuertes, F., Iglesias-Caballero, M., Monzón, S., Jiménez, P., Varona, S., Cuesta, I., Zaballos, Á., Thomson, M. M., Jiménez, M., García Pérez, J., Pozo, F., Pérez-Olmeda, M., Alcamí, J., and Casas, I. (2020). Phylodynamics of sars-cov-2 transmission in spain. bioRxiv.

Eichenbaum, M. S., Rebelo, S., and Trabandt, M. (2020). The macroeconomics of epidemics. Working Paper 26882, National Bureau of Economic Research.

Farboodi, M., Jarosch, G., and Shimer, R. (2020). Internal and external effects of social distancing in a pandemic. Working Paper 27059, National Bureau of Economic Research.

Fogli, A., Perri, F., Ponder, M., and Azzimonti, M. (2020). Pandemic control in econ-epi networks. Technical Report 690.

Galor, O. and Weil, D. N. (2000). Population, technology, and growth: From malthusian stagnation to the demographic transition and beyond. American Economic Review, 90(4):806–828.

Glover, A., Heathcote, J., Krueger, D., and Ríos-Rull, J.-V. (2020). Health versus wealth: On the distributional effects of controlling a pandemic. Working Paper 27046, National Bureau of Economic Research.

Greenwood, J., Seshadri, A., and Vandenbroucke, G. (2005). The Baby Boom and Baby Bust. American Economic Review, 95(1):183–207.

Iorio, D. and Santaeulàlia-Llopis, R. (2016). Education, HIV Status, and Risky Sexual Behavior: How Much Does the Stage of the HIV Epidemic Matter? Working papers, Barcelona Graduate School of Economics.

Kaplan, G., Moll, B., and Violante, G. (2020). Pandemics according to HANK. Technical report.

Lee, S. Y., Lei, B., and Mallick, B. (2020). Estimation of COVID-19 spread curves integrating global data and borrowing information. PloS ONE, 15(7):1–17.

Loannidis, J. (2020). Infection fatality rate of covid-19 inferred from seroprevalence data. Technical Report 20.

Lucas, R. E. (2004). The Industrial Revolution: past and future. Annual Report, 18(May):5–20.

Piguillem, F. and Shi, L. (2020). Optimal COVID-19 Quarantine and Testing Policies. Technical report.

Pollan, M., Perez-Gomez, B., Pastor-Barriuso, R., Oteo, J., Hernan, M. A., Perez-Olmeda, M., Sanmartin, J. L., Fernandez-Garcia, A., Cruz, I., de Larrea, N. F., Molina, M., Rodriguez-Cabrera, F., Martin, M., Merino-Amador, P., Paniagua, J. L., Munoz-Montalvo, J. F., Blanco, F., and Yotti, R. (2020). Prevalence of SARS-CoV-2 in Spain (ENE-COVID): a nationwide, population-based seroepidemiological study. Technical report.

A From Deaths to Active Infections

We show that the dynamics of an epidemic (including new and active infections) can be tracked using the flow of deaths. With some assumptions on the overall fatality rate and on the arrival process of deaths (and recoveries), the (unobserved) number of new and active infections at any time can be directly backed out from the flow of deaths.

Consider a scenario in which a virus that infects a flow $X_{i,t}$ of individuals at time t is expected to be deadly for a proportion ζ of those individuals, who otherwise recover. Assume that the death process is known. That is, ζ denotes the fatality rate of the virus. Specifically, assume the true timing of death for the infected individuals is random and follows a Poisson process. That is, at the time of infection, the time (and event) of death is uncertain at the individual level, but the average time from infection to death, τ_D, is known, say twelve days.[24] Then, the expected total number of deaths in $\tau_D = 12$ days is

$$E[X_{D,t+\tau_D}] = \lambda_t$$

where $\lambda_t = \zeta X_{i,t}$ is a time-varying Poisson parameter and ζ is the fatality rate. In this context, if the flow of deaths per period follows an observed time series $\{X_D\}_{t=12}^{T}$ as depicted in panel (a) of Figure 9, we can recover the expected number of new infections that occurred twelve days earlier using the Poisson process. That is, given a fatality rate ζ we can recover the flow of new infections that deliver the observed flow of deaths by solving for the series $X_{i,t}$ in

$$X_{D,t+\tau_D} = \zeta X_{i,t}. \tag{14}$$

In panel (c) of Figure 9, we plot the series of new infections $\{X_{i,t}\}_{t=0}^{T-\tau_D}$ associated with the observed flow of deaths $\{X_{D,t}\}_{t=\tau_D}^{T}$ assuming $\tau_D = 12$ and $\zeta = 0.00025$.[25] With the assumed homogeneous arrival rate of deaths, the time lag between the peaks of the backed out flow of infections and the given flow of new deaths corresponds to the average time from infection to death τ_D.[26] The accumulated deaths, D_t, associated with the observed flow of deaths and accumulated new infections, i_t, associated with the backed out flow of new infections are shown in

[24] Recently, the Robert Koch Institute in Germany reported an average of approximately 30 days from infection to death in the case of Covid-19, see here.

[25] Although the Covid-19 fatality rate remains relatively unknown even up to this date, its estimates tend to range between 0.001% and 1.54% (Loannidis, 2020). In our illustration, we choose $\zeta = 0.025\%$ which implies a 4.5% seroprevalence rate at $t = 84$. This is in line with the 4.6% seroprevalence rate (from PCR tests) as well as with the self-reported Covid-19 symptoms for Spain from data collected 84 days after the country started reporting active infections (Pollan et al., 2020).

[26] This would change if the estimated arrival of deaths were to differ over time, e.g., because of systematic changes in the infected population and heterogeneous death processes across those subgroups, say by age or health status.

Figure 9: An Illustration of an Epidemic

Deaths, D_t

(a) Flow: $X_{D,t}$ (b) Stock: D_t

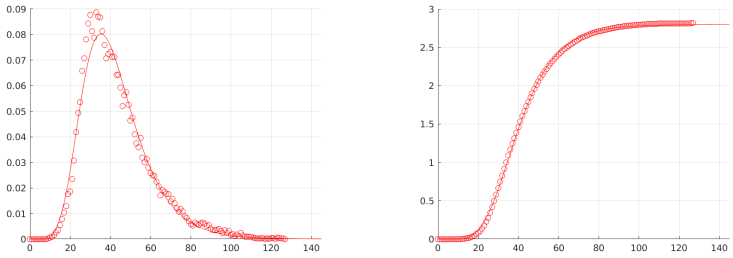

New Infections, i_t, and Recoveries R_t

(c) Flow: $X_{i,t}$ and $X_{R,t}$ (d) Stock: i_t and R_t

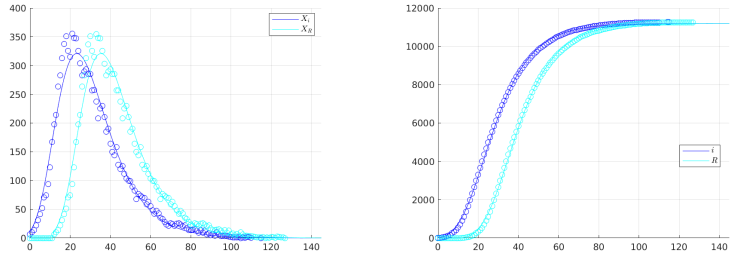

Active Infections, I_t

(e) Flow: $X_{I,t}$ (f) Seroprevalence: I_t/POP_t

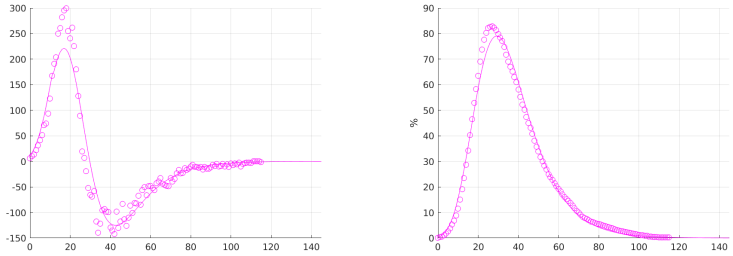

Notes: Panel (a) and panel (b) show respectively the 'observed' flow and stock of deaths for Spain. The unobserved flows of new infections, recoveries and prevalence are tracked using the population law of motions defined by equations (14)-(16) in Section A. For our illustration we use a fatality rate of $\zeta = 0.025\%$ and $\tau_R = \tau_D = 12$. All panels on Figure 9 are expressed $\times 10000$, except panel (f) that shows the seroprevalence of the disease as the percentage of active infections in the population, with the current estimate for the population of Spain being around 47 million. Smoothed lines are based on predicted values of a generalized logistic function estimated on the flow of deaths data. *Source:* Instituto de Salud Carlos III.

panels (b) and (d) of Figure 9, respectively.

Along the same lines, note that given the fatality rate and the backed out flow of new infections, it is straightforward to further back out the flow of recovered individuals, $X_{R,t}$, if the

time between infection and recovery, τ_R, is known:

$$X_{R,t+\tau_R} = (1-\zeta)X_{i,t} \tag{15}$$

In this manner, using an average time of recovery of $\tau_R = \tau_D = 12$ days, we can use equations (14) and (15) to find, $X_{R,t} = X_{i,t-12} - X_{D,t}$. Under these assumptions, we plot the flow of recovered population, $X_{R,t}$ and its associated stock, R_t, respectively, in panel (c) and (d) of Figure 9.[27]

Furthermore, note that the flow of the actively infected population at any point in time does not only need to take into account the flow of new infections but also the outflow from those individuals that either recover or die. In this manner, we can recover the series of the flow of active infections in period t, $X_{I,t}$, as the flow of new infections in that period minus the flow of recoveries and the flow of deaths in that period as

$$X_{I,t} = X_{i,t} - (X_{R,t} + X_{D,t})\,. \tag{16}$$

Given the series $X_{I,t}$ we can recover the associated stock of actively infected individuals, I_t, in the population. We show the flow active infections in panel (e) of Figure 9. In panel (f) we show the percentage of active infections in the population, POP_t, which results in a seroprevalence of 4.5% and 0.85% for $t = 84$ and $t = 104$ respectively.[28]

A relevant aspect of our illustration is that in order to estimate the flow of infections we do not require knowledge on the process through which infections occur. Note that this does not limit our ability to recover the infection rate either: if the amount of susceptible population to infection is known (e.g., the entire population is susceptible) then the estimated flow of deaths pins down the infection rate of the susceptible population understood as the proportion ω_t of susceptible population S_t that at any given period get infected, i.e., ω_t is the only unknown in $X_{i,t} = \omega_t S_t$.

B Estimating the Generalized Logistic Function

B.1 Approach

We find that the GLF prediction smooths the time series data of both the flow of deaths and the stock of deaths tracking well their main features. This is the case for both the nationwide time

[27] Those with mild cases of Covid-19 appear to recover within one to two weeks. For severe cases, recovery may take six weeks or more, see here: Hopkins Medicine. For this illustration we use an average time of recovery of twenty-one days.

[28] These numbers are in line with the results presented by Pollan et al. (2020) for Spain.

Table 4: GLF Estimates

	Spain	Madrid	Rest of Spain
β_0	0.56	1.14	0.67
	[0.56 , 0.62]	[1.14 , 1.34]	[0.68 , 0.78]
β_1	0.09	0.11	0.12
	[0.08 , 0.09]	[0.09 , 0.01]	[0.09 , 0.11]
β_2	41.33	37.42	42.50
	[42.30, 41.69]	[39.54 , 38.50]	[44.55 , 43.32]
β_3	0.07	0.09	0.27
	[0.03 , 0.05]	[0.04 , 0.07]	[0.11 , 0.18]

Notes: Table shows the Bootstrapped 90% confidence bounds in parenthesis.

series (panel (a) in Figure 4) as well as for Madrid and the rest of Spain (panel (b) in Figure 4). First, note that our estimation is able to capture the accumulated number of deaths in Spain as well as the significantly higher death toll (per million inhabitants) in Madrid compared to the rest of Spain. These results are driven by our estimated value of β_0 that is 0.56 nationwide, 1.14 for Madrid and 0.5279 for the rest of Spain. Second, the GLF also captures a significantly faster average growth (and decline) of the flow of deaths in the rest of Spain than in Madrid as per the estimates of β_1 that are, respectively, 0.14 and 0.10. Third, our parametrization is able to capture the asymmetry by which the flow of deaths increase at a faster pace compared with the pace at which it decreases. In particular, Madrid shows an estimated asymmetry that is significantly larger than the asymmetry in the rest of Spain with estimates of β_3 of, respectively, 0.088 and 0.375. Finally, note that the estimated values of β_2 confirm that Madrid reaches the maximum of deaths earlier than the rest of Spain.

B.2 Bootstrapping

To draw bootstrap samples of standard errors, we first extract standard errors by estimating a regression on log flows of deaths

$$\min_{\boldsymbol{\beta^d}} \frac{1}{2} \sum_{t=t_r^0}^{T(\tau)} \left(\ln\left(y_{tr}\right) - \ln\left(X_{D,t}(\boldsymbol{\beta_r^a})\right)\right)^2$$

and compute predicted errors from the log difference

$$\hat{\epsilon}_{tr} = \ln\left(y_{tr}\right) - \ln\left(X_{D,t}(\hat{\boldsymbol{\beta}}_r^{\boldsymbol{d}})\right).$$

We draw bootstrap samples of these predicted residuals to compute bootstrap samples of flows of deaths, which we sum up to generate bootstrap samples of the stock of deaths. When drawing the bootstrap samples of error terms we take both cross-sectional dependence and autocorrelated errors into account by drawing in each bootstrap iteration the same index sequence of error terms and by a blockwise bootstrap, where we choose a block length of 4.[29] We take into account potential changes in the error structure before and after the policy reform date at $t_p + \tau$ by conducting the blockwise bootstrap within the two time blocks $[t_0(r), \ldots, t_p + \tau - 1]$ and $[t_p + \tau, \ldots, T(\tau)]$. Bootstrap samples in bootstrap iteration b of the flow of death are constructed from the bootstrap errors ϵ_{tr}^b as

$$\ln y_{tr}^b = \ln \left(X_{D,t}(\hat{\boldsymbol{\beta}}_r^{\boldsymbol{d}}) \right) + \epsilon_{tr}^b$$

Summing up over time gives an according bootstrap sample for the stock of deaths Y_{tr}^b.

C Predicting Lives Saved in Madrid

Figure 10 shows the log of the policy effect estimate $\hat{\gamma}_r^p$ by stage of the epidemic by regions and the prediction for Madrid, cf. equation (13).

[29] According to the standard rule of thumb that the blocklength should relate to the overall sample size as $n \approx T^{\frac{1}{3}}$.

Figure 10: Policy Effect Estimate $\hat{\gamma}$ by Stage of Epidemic [in Logs]

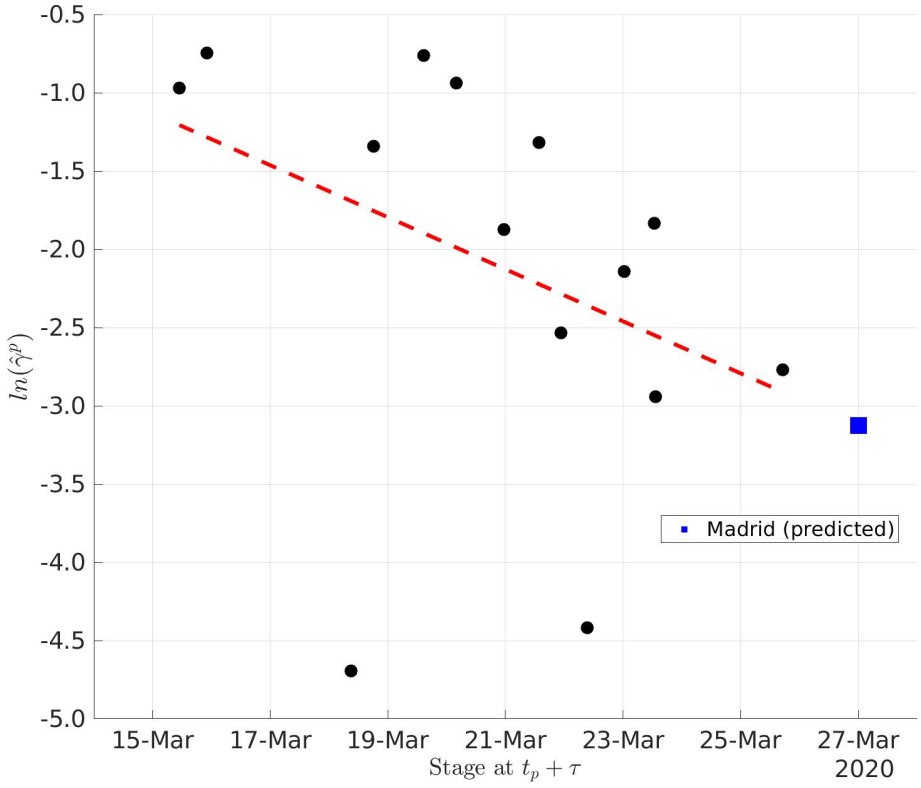

Notes: Log of policy effect estimate $\ln(\hat{\gamma}^p)$ by stage of the epidemic and prediction for Madrid.

Recent Issues

No. 293	Christoph Hambel, Holger Kraft, André Meyer-Wehmann	When Should Retirees Tap Their Home Equity?
No. 292	Andrea Modena	Recapitalization, Bailout, and Long-run Welfare in a Dynamic Model of Banking
No. 291	Loriana Pelizzon, Satchit Sagade, Katia Vozian	Resiliency: Cross-Venue Dynamics with Hawkes Processes
No. 290	Nicola Fuchs-Schündeln, Dirk Krueger, Alexander Ludwig, Irina Popova	The Long-Term Distributional and Welfare Effects of Covid-19 School Closures
No. 289	Christian Schlag, Michael Semenischev, Julian Thimme	Predictability and the Cross-Section of Expected Returns: A Challenge for Asset Pricing Models
No. 288	Michele Costola, Michael Nofer, Oliver Hinz, Loriana Pelizzon	Machine Learning Sentiment Analysis, COVID-19 News and Stock Market Reactions
No. 287	Kevin Bauer, Nicolas Pfeuffer, Benjamin M. Abdel-Karim, Oliver Hinz, Michael Kosfeld	The Terminator of Social Welfare? The Economic Consequences of Algorithmic Discrimination
No. 286	Andreas Hackethal, Michael Kirchler, Christine Laudenbach, Michael Razen, Annika Weber	On the (Ir)Relevance of Monetary Incentives in Risk Preference Elicitation Experiments
No. 285	Elena Carletti, Tommaso Oliviero, Marco Pagano, Loriana Pelizzon, Marti G. Subrahmanyam	The COVID-19 Shock and Equity Shortfall: Firm-Level Evidence from Italy
No. 284	Monica Billio, Michele Costola, Iva Hristova, Carmelo Latino, Loriana Pelizzon	Inside the ESG Ratings: (Dis)agreement and Performance
No. 283	Jannis Bischof, Christian Laux, Christian Leuz	Accounting for Financial Stability: Bank Disclosure and Loss Recognition in the Financial Crisis
No. 282	Daniel Munevar, Grygoriy Pustovit	Back to the Future: A Sovereign Debt Standstill Mechanism IMF Article VIII, Section 2 (b)